

The illusion of personal health decisions for infectious disease management: disease spread in social contact networks

Matthew Michalska-Smith^{1,2}, Eva A Enns³, Lauren A White⁴, Marie L J Gilbertson⁵, and Meggan E Craft¹

¹Department of Ecology, Evolution and behaviour, University of Minnesota, USA

²Department of Plant Pathology, University of Minnesota, USA

³School of Public Health, University of Minnesota, USA

⁴National Socio-Environmental Synthesis Center, University of Maryland, USA

⁵Veterinary Population Medicine Department, University of Minnesota, USA

March 2, 2023

Abstract

2 Close contacts between individuals provide opportunities for the transmission of diseases, including COVID-19.
3 19. Individuals take part in many different types of interactions, including those with classmates, co-workers,
4 and household members; the conglomeration of all of these interactions produces a complex social contact
5 network interconnecting individuals across the population. Thus, while an individual might decide their own
6 risk tolerance in response to a threat of infection, the consequences of such decisions are rarely so confined,
7 propagating far beyond any one person. We assess the effect of different population-level risk-tolerance
8 regimes, population structure in the form of age and household-size distributions, and different interaction
9 types on epidemic spread in plausible human contact networks to gain insight into how contact network
10 structure affects pathogen spread through a population. In particular, we find that behavioural changes
11 by vulnerable individuals in isolation is insufficient to reduce those individuals' infection risk and that
12 population structure can have varied and counter-acting effects on epidemic outcomes. The relative impact
13 of each interaction type was contingent on assumptions underlying contact network construction, stressing
14 the importance of empirical validation. Taken together, these results promote a nuanced understanding of
15 disease spread on contact networks, with implications for public health strategies.

16 1 Introduction

17 Many respiratory diseases, including influenza, tuberculosis, and COVID-19, are primarily transmitted
18 through close contact between an infectious individual and a susceptible one, whether by direct physical
19 contact or through expelling contaminated droplets via coughing, sneezing, or breathing [1]. While not all
20 such interactions lead to a transmission event, the transmission network (*i.e.* the actual set of who infects
21 whom in a population) is a subset of this wider contact network (*i.e.* the set of all interactions between
22 individuals that could result in in disease transmission) [2].

23 The importance of interpersonal contact for disease dynamics has been recognized for centuries, with
24 isolation of infected individuals being recorded in fifteenth century Italy [3], and has become more formalized
25 in recent decades [4, 5, 6]. Yet, detailing the specific ways in which the structure of contact networks relates
26 to differences in disease spread between populations has been hampered by the size and complexity of human
27 social networks, which are an agglomeration of many different kinds of interpersonal interactions [7]. A given
28 person, for instance, will interact with some people at home (their family or housemates), others when they
29 go to work (co-workers and colleagues), and yet others when they go to the local store for groceries (neighbors
30 and strangers). Not only do the individuals involved in each of these sub-networks differ for any given person,
31 but also the structure and intensity of interactions might likewise differ between contexts.

32 Pathogens spread differently in different localities in part because of a difference in social contact network
33 structure [8, 9, 10, 6], thus we might also expect disease dynamics to vary across social contexts: to spread
34 differently at work than at school, through a home than through a neighbourhood. Yet, unlike the case of
35 two distinct localities, these layers of interactions are also not independent from one another, linked by the
36 individuals that take part in multiple layers. It is the combination of these layers into an integrated network
37 detailing all possible infection pathways that affects the ultimate spread of disease through a population. But
38 how much does each type of interaction contribute to this final disease spread? Can the layers be modified
39 independently in order to alter a population's risk in the face of disease spread?

40 Operationalizing the connection between contact network structure and disease spread, public health
41 interventions such as travel restrictions, business and school closures, and individual isolation and/or quar-
42 antining seek to reduce disease spread through direct modification of the contact network [11, 12]. In short,
43 such modifications seek to sever potential infection pathways through the contact network before they are
44 realized, limiting the number of potential secondary cases available to a given infectious individual. These ap-
45 proaches can range from hyper-local—only isolating individuals who have been confirmed to be infected—to
46 society-wide—wholesale economic lockdowns and *cordons sanitaire* [13].

47 In their initial response to the COVID-19 pandemic, many countries imposed strict restrictions on social
48 interactions—especially those within schools and workplaces [14]—with the goal of limiting disease spread
49 through the mass fragmentation of societal contact networks [15]. While such efforts have, in general, been
50 found to be effective both historically [16], and in the current pandemic [17, 18], they are nevertheless
51 a blunt intervention. More restrained approaches, such as test-trace-quarantine can be more surgical in
52 their application, but their efficacy tends to be limited by insufficient participation and high costs when
53 cases are surging [4, 19, 20]. A middle ground could involve restricting certain types of interactions while
54 leaving others unaffected, balancing disease mitigation and socio-economic hardship (*e.g.* closing schools, but
55 leaving workplaces open, or *vice versa*). Finally, not all public health interventions seek to completely sever
56 edges in the contact network. Softer approaches, such as masking, increased attention to personal hygiene,
57 improved ventilation, and physical distancing can be used to reduce the strength of interactions, *i.e.* reduce
58 the transmission rate given interaction between two individuals, rather than eliminating the interaction
59 altogether [21, 22].

60 In addition to differences between types of interactions, which might be relatively consistent from one
61 individual to another, there are also differences between individuals both in behaviour [23, 24] and in un-
62 derlying health conditions that increase the likelihood of experiencing adverse health outcomes in the event
63 of infection [25]. While a decision might be made on a personal level (*e.g.* one person might decide to return
64 to in-person work, while another might take advantage of a work-from-home option), the consequences of
65 this decision have the potential to propagate far beyond a focal individual, with individuals serving as either
66 bridge or firewall in a pathogen’s infection chain.

67 In this work, we investigate the impact of plausible human contact network structure [26, 7, 13] on the
68 spread of disease across three scales of network structure, using COVID-19 as an example. First, we consider
69 differences in individual risk tolerance with respect to an individual’s contact with persons in the network
70 who are at greater risk of adverse outcomes following infection (*i.e.* “vulnerable” individuals). Second, we
71 consider the effect of wider population structure on the spread of disease, comparing two locales that differ in
72 age- and household-size distributions. Finally, we add to these two considerations the relative contribution
73 of two layers in the contact network (*i.e.* interactions between classmates at school and interactions between
74 co-workers at work). We focus on these two layers in particular as they (along with household interactions)
75 comprise the majority of potential transmission events in modern society [27, 28], and have been the focus
76 of prior research and public health interventions, better allowing us to contextualize any results [20, 14,
77 13, 29]. Taken together, the results of this investigation provide a foundation for better understanding the

78 role of contact network structure on the spread of disease, and an avenue for better targeting public-health
79 interventions to limit further disease spread.

80 **2 Methods**

81 **2.1 Network construction**

82 We constructed human contact networks by sequentially adding interaction layers to a base network of
83 individuals grouped into households according to United States (US) 2019 American Community Survey
84 data on the distribution of household sizes [30]. Each individual was assigned an age (according to US
85 2019 American Community Survey data [31]) and a binary “vulnerable” status. Vulnerability was assigned
86 according to age-adjusted hospitalization rates [32]. School-age children were then assigned to classrooms
87 (using an approximate classroom size of 20 students), and pre-retirement-age adults (accounting for US
88 unemployment rates) to workplaces (according to a modified distribution of US business sizes). To make
89 our networks more realistic, we additionally considered the effect of community spread of disease outside
90 of the structured settings of work and school (*e.g.* spread at the grocery store or local shopping center).
91 For this, we added a layer connecting all individuals in the network to all others at a low transmission rate
92 (*i.e.* “background transmission”).

93 Each of these four network layers is a collection of distinct, fully connected sub-networks that correspond
94 to households, classrooms, workplaces, or the community as a whole. By layering these networks together,
95 the isolated clusters from any one layer become intertwined through the connections in other layers. For
96 example, a student might be connected to an unrelated, vulnerable adult through an interaction chain
97 involving a classmate interaction with a friend, a household interaction between the friend and their parent,
98 and a workplace interaction between the parent and an elderly co-worker. The strength of interaction in
99 the co-worker and classmate interaction layers was varied systematically to explore the relative importance
100 of each of these layers, while those in the household layer (as well as background transmission) were held
101 constant.

102 We considered two US states as case studies for comparing differences in local population structure.
103 Using US 2019 American Community Survey data (see Electronic Supplementary Material section S1 for de-
104 tailed data sources), we constructed synthetic networks with age- and household-size distributions matching
105 those of either Florida—a US state with a relatively high average age and small average household size—or
106 Texas—a US state with a relatively low average age and large average household size (Electronic Supple-

Table 1: Summary statistics for networks generated for each of the two localities used in the main text.

Metric	“Florida” mean (sd) ¹	“Texas” mean (sd) ¹
Number of individuals	3 001	3 000
Number school-age	503 (20.5)	648 (22.5)
Number employed	1 549 (27.4)	1 595 (27.5)
Number vulnerable	628 (22.2)	535 (20.9)
Number of households	1 212	1 056
Number households with children	462 (15.1)	517 (13.4)
Number of households with vulnerable	508 (16.3)	423 (14.9)
Total number of edges (no contact avoidance) ²	24 961 (611.1)	28 411 (578.5)
Household edges	3 425	4 519
Classmate edges	5 890 (307.7)	7 744 (345.0)
co-worker edges	15 646 (593.2)	16 148 (560.5)
Edges when vulnerable individuals avoid work/school interactions	17 655 (564.1)	20 766 (570.6)
Edges when members of vulnerable households avoid interactions	7 857 (539.2)	8 605 (610.1)

¹ Values are presented with both mean and standard deviation except when there was no variance, in which case the constant value is presented.

² “Background” transmission edges are omitted from this (and other edge) count(s). Because they connect every individual to every other, there are always $N(N - 1)/2$ such edges, where N is the number of individuals in the network.

107 *mentary Material section S2 and fig. S1).* Each network was further populated with classmate and co-worker
 108 interaction layers, as detailed above, using the same algorithm and parameters for both localities. Networks
 109 were generated to have approximately the same number of individuals (3 000), which necessitates a different
 110 number of households in each network due to the aforementioned differences in average household size.

111 Finally, we modified the above networks according to three risk-tolerance scenarios, generalizing be-
 112 haviours to all individuals in the population. First, we considered a population in which all individuals,
 113 regardless of inherent vulnerability, behave identically, fully participating in their co-worker and classmate
 114 interactions. Second, we considered a case where vulnerable individuals avoid those interactions (*i.e.* do not
 115 go to work/school and therefore have no co-worker or classmate interactions) in order to reduce their own
 116 exposure risk. Finally, we considered a case where all members of any household containing at least one
 117 vulnerable individual avoid co-worker and classmate interactions in an effort to reduce exposure to their
 118 vulnerable housemates. In all three scenarios, background and household interactions were left unchanged.
 119 Table 1 details differences between the networks constructed for each of the two locales and under different
 120 risk-tolerance scenarios.

121 **2.2 Disease simulation**

122 Pathogen spread through the population was simulated according to modified SEIR dynamics, using a
123 discrete-time, chain binomial model [33]. Specifically, individuals (nodes) in the network fell into one of
124 six classes at each timestep: susceptible to infection (S), exposed but not yet infectious (E), infectious
125 and symptomatic (I_s), infectious and asymptomatic (I_a), recovered and immune to future infection (R), or
126 a victim of disease-induced mortality (D). Transitions between classes were governed by rate parameters
127 (table 2) that, when appropriate, could take two discrete values based on an individuals' inherent vulnerability
128 to severe disease.

129 Explicitly, susceptible nodes can be infected at each timestep depending on their network connections:

$$S \xrightarrow{\beta_x^{j,i}} E.$$

130 Where $\beta_x^{j,i}$ is the rate of transmission between two nodes, one infectious (i) and one susceptible (j),
131 connected by interaction type x . A susceptible individual will have the chance to be infected by each of
132 their infectious interaction partners on each timestep. We considered three alternative rates of background
133 transmission (table 2), but only present figures corresponding to a value of $\beta_{background} = 0.001/N$ (where N
134 is the number of nodes in the network) in the main text. See Electronic Supplementary Material section S3
135 for figures corresponding to values of 0 and 0.05/ N .

136 Exposed individuals' experience disease progression at a constant rate:

$$E \xrightarrow{\sigma*\rho} I_s, E \xrightarrow{\sigma*(1-\rho)} I_a.$$

137 Where σ represents the disease progression rate (the inverse of the time between becoming infected and
138 becoming infectious) and ρ is the proportion of infected individuals that develop symptoms. Infectious
139 individuals recover or die at constant rates (depending on their symptomaticity and inherent vulnerability):

$$I_s \xrightarrow{(1-\frac{2}{3}\delta(i))\gamma} R, I_a \xrightarrow{(1-\frac{2}{3}\delta(i))\gamma} R, I_s \xrightarrow{\mu+\delta(i)\nu} D$$

140 Where $\delta(i)$ is an indicator function that returns 1 if an individual is vulnerable, and 0 otherwise, γ
141 represents the rate of recovery, which is (approximately three times) longer for vulnerable individuals [34,
142 35], μ represents a baseline mortality rate, and ν represents additional mortality experienced by vulnerable
143 individuals. All disease parameters were set to literature values approximated for the initial wave (original

Table 2: Estimates and description of parameters for the SARS-CoV-2 model used in this work.

Parameter	Description	Point Estimate*	Reference(s)
$\beta_{background}$	The transmission rate for community interactions	0, $0.001/N$, or $0.05/N$	
$\beta_{household}$	The transmission rate for interactions between household members	0.13	Rosenberg et al. [36], Bar-On et al. [37]
$\beta_{classmate}$	The transmission rate for interactions between classmates	none [†]	
$\beta_{co-worker}$	The transmission rate for interactions between co-workers	none [†]	
σ	The incubation period (the inverse of the average latent period duration)	1/5.5	Bar-On et al. [37]
ρ	Proportion of new infectious individuals that are symptomatic	0.35 [‡]	Wang et al. [38], Bar-On et al. [37]
γ	The recovery rate (the inverse of the average duration of the infectious period)	1/4.5	Bar-On et al. [37]
μ	Baseline mortality rate for symptomatic, non-vulnerable individuals	1/27 000	The World Bank [39], Ugarte et al. [40]
ν	Additional mortality due to vulnerability	1/1 000	Bar-On et al. [37]

* Units are days^{-1} unless otherwise noted; N signifies the number of individuals in the network.

† values sampled from $10^{[-3, -0.5]}$ (one for each transmission rate per simulation), where $[a, b]$ represents a range from a to b (inclusive) from which values were uniformly randomly sampled.

‡ this value is unit-less

¹⁴⁴ Wuhan strain) of COVID-19 (table 2).

¹⁴⁵ Note that we assume: 1) per-contact transmission rates are independent of the symptomaticity of the
¹⁴⁶ infectious interaction partner, 2) all mortality is disease induced, and 3) that only symptomatic individuals
¹⁴⁷ suffer disease-induced mortality.

¹⁴⁸ Populations were seeded with a single (randomly selected) infected individual and simulations were
¹⁴⁹ allowed to run until no further infections were possible. A total of 10 000 unique combinations of classmate
¹⁵⁰ ($\beta_{classmate}$) and co-worker ($\beta_{co-worker}$) transmission rates were sampled using a Latin-Hypercube approach
¹⁵¹ [41], each parameter combination was run for each of the two localities and three risk-tolerance regimes,
¹⁵² leading to a total of 60 000 simulated epidemics.

¹⁵³ 2.3 Epidemic outcome quantification

¹⁵⁴ Epidemic spread was quantified using the total number of individuals infected, the total number of vul-
¹⁵⁵ nerable individuals infected, the average number of individuals concurrently infectious, the total number of
¹⁵⁶ individuals that died, the maximum number of concurrently infectious individuals, the number of timesteps
¹⁵⁷ to reach that peak, the number of timesteps that passed before the first vulnerable individual was infected,

158 the percentage of vulnerable households (*i.e.* households with at least one vulnerable member) that escape in-
159 fection, and the timepoint with the highest number of deaths in the simulation (full definitions of each metric
160 and correlations between metrics available in the Electronic Supplementary Material section S4 and fig. S10).
161 This last metric could be considered a proxy for the anticipated time until peak hospital demand. While we
162 only present a subset of these in the main text, all outcomes can be viewed in the Electronic Supplementary
163 Material(in particular section S5 for those corresponding to the main text parameterization). Epidemi-
164 logical outcome variables were, in general log-transformed prior to analysis, and normalized according to
165 relevant aspects of network size when comparing between locales.

166 All simulations were conducted in C++ version 8.1.0, with data manipulation and plotting done in R
167 version 4.2.0 [42]. For specific packages used, see Electronic Supplementary Material section S6. Code
168 to replicate all aspects of these analyses is available online: https://github.com/mjsmith037/Layered_Interactions_COVID_Model.

170 3 Results & discussion

171 3.1 Quantifying the effect of differential risk-tolerance behaviour

172 As expected, increasing the transmission rate for classmates or co-workers increased the number of sec-
173 ondary infections in an otherwise fully susceptible population (the reproduction number R_0), the number
174 of infectious individuals, the number of vulnerable people infected and the total number of individuals that
175 died (fig. 1). Yet, for this effect was modulated by behaviour: in particular, we found that the actions of
176 vulnerable individuals in isolation marginally reduced the total disease burden on the population in terms of
177 number of cases and deaths, except when transmission rates were already low. However, there was a substan-
178 tial reduction in these values when household members likewise avoided work/school interactions themselves
179 from other individuals in the network (fig. 1). Specifically, considering only simulations in which at least
180 5% of the population is infected (*i.e.* an epidemic occurs), for a given pair of classmate and co-worker trans-
181 mission rates, we see an average reduction in peak number of infectious individuals of 42% when vulnerable
182 individuals reduce their contacts, but a reduction of 77% when entire households reduce interactions. For
183 deaths, a reduction of 41% when individuals reduce interactions, but over 99% when households also reduce
184 their interactions. In contrast, R_0 showed less difference between risk-tolerance regimes, decreasing by two
185 individuals (on average) when individuals isolated, but three individuals when households also reduced their
186 interactions.

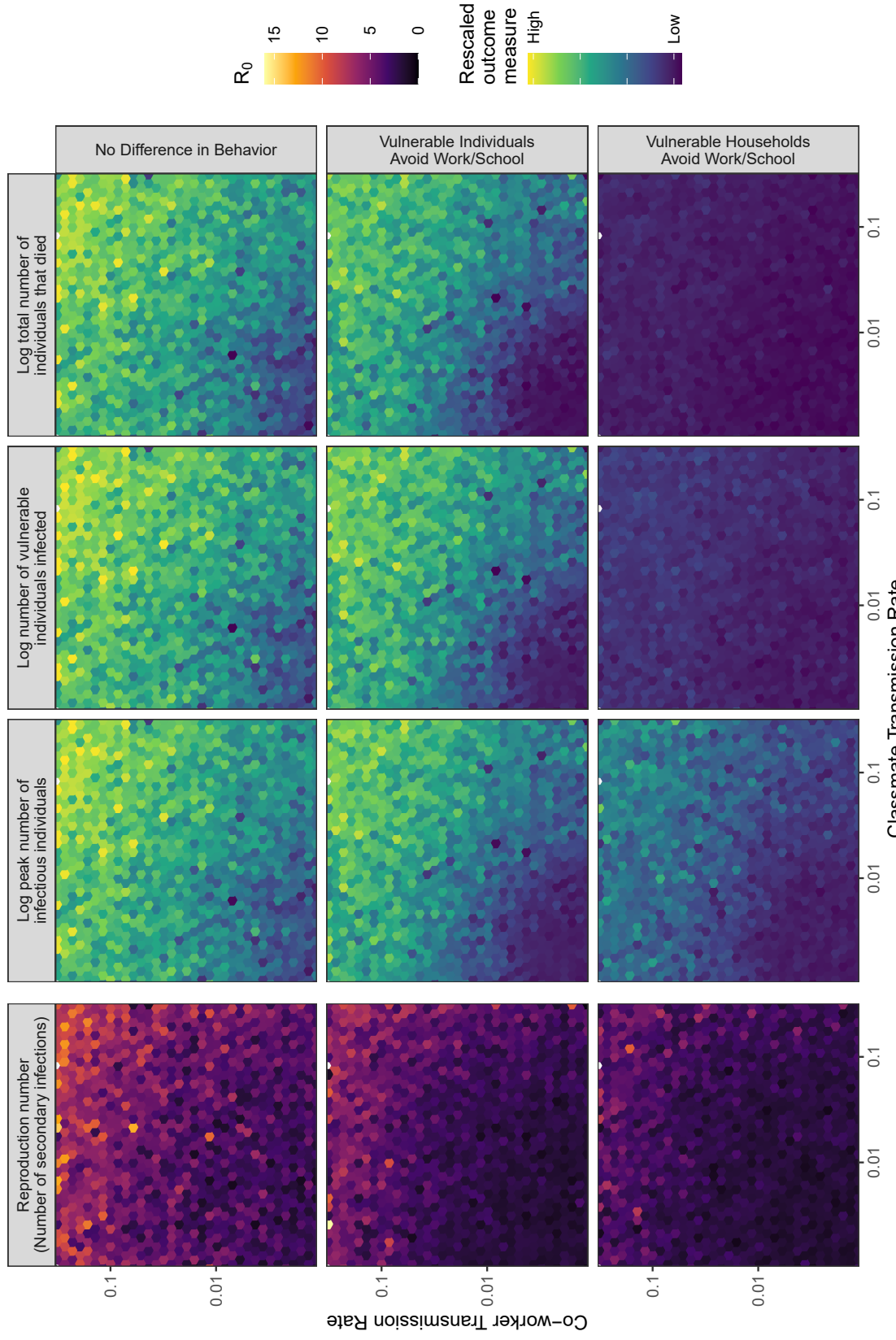


Figure 1: Relative epidemic outcome (columns), quantified as the reproduction number (leftmost), peak number of individuals infected (center-left), the number of vulnerable individuals infected (center-right), or the total number of individuals that died (rightmost) over the course of the simulation. Individuals in the network either (rows): did not change behaviour in response to (contact with individuals with) vulnerability status (top), changed behaviour if they were vulnerable themselves (middle), or changed behaviour when a member of their household was vulnerable (bottom). Values (other than the reproduction number) were log-scaled and normalized for each epidemic outcome such that the maximum value is 1 (yellow) and the minimum value is 0 (purple). Multiple points within each hexagon were averaged to produce the plotted value. Each panel consists of a heatmap showing the relative epidemic outcome of simulations spanning various levels of co-worker (vertical axis) and classmate (horizontal axis) transmission. Maximum disease burden in all cases occurs when the transmission rates are both high (top right corners of each panel), while the disease tends to die out with minimal cases and death when both rates are low (bottom left of each panel). Results here are aggregated across local population structures, which were qualitatively similar. See Electronic Supplementary Material section S3 and figs. S2, S5, S6 and S9 for analogous figures under different background transmission rates and fig. S11 for alternative epidemiological outcome measures.

187 This trend was consistent across other metrics of epidemiological outcomes, such as, the number of
188 vulnerable individuals infected and the time until the first vulnerable individual is infected (Electronic Sup-
189 plementary Material fig. S11). Likewise, we saw consistency across a range of transmission rates between
190 classmates and between co-workers. Importantly, however, if background transmission rates are high enough,
191 classmate and co-worker transmission is rendered irrelevant, precluding any substantial differences between
192 behaviour treatments (average reductions in total mortality of 3% and 7%, for individuals and households
193 reducing interactions, respectively; Electronic Supplementary Material fig. S6). These patterns were con-
194 sistent across local population structures (*i.e.* Texas or Florida), so we aggregated results across locales
195 for figs. 1, S2, S5, S6, S9 and S17. Additionally, these patterns were robust to alternative assumptions
196 of network construction, for instance, the implementation of age-structured weighted of transmission rates
197 (average reductions in total mortality of 12% and 79%, for individuals and households reducing interactions,
198 respectively; Electronic Supplementary Material section S7 and fig. S14). Interestingly, these effects in
199 the age-structured case occurred despite almost no change in R_0 between risk-tolerance regimes (Electronic
200 Supplementary Material fig. S16).

201 We emphasize that the reduction in prevalence and mortality that we see when removing edges associated
202 with decreased risk tolerance is not a product of reducing the number of interactions in the network, *per*
203 *se*. Performing additional simulations in which the same number of edges from each interaction layer in
204 the network is removed as in the risk-tolerance regime simulations described above, but choosing which
205 edges within each layer to remove at random (*i.e.* irrespective of an individuals (contact with) vulnerable
206 individuals), yields no substantial difference between link-removal treatments (average reductions in peak
207 prevalence of 3% and 15%, for individuals and households reducing interactions, respectively; section S8
208 and fig. S17). Put another way, it is not *how many* edges are removed, but rather *which* edges are removed
209 that is critical for effective disease management.

210 The absence of reduced disease burden when only vulnerable individuals change their behaviour can
211 be attributed, at least in part, to the high-interaction strength expected for within-household interactions,
212 limiting the efficacy of contact-reduction for vulnerable individuals sharing households with less vulnerable
213 individuals. Unless the whole household takes actions to reduce their exposure, we see limited benefits
214 of reducing a particular individuals exposure in isolation. This is true even if we only look at the rates
215 of infection in the vulnerable individuals themselves. Moreover, because the vast majority of deaths from
216 COVID-19 are individuals with underlying health conditions that provide an inherent vulnerability to adverse
217 outcomes [43], reducing the number of vulnerable individuals infected has a direct effect of reducing mortality

218 as well.

219 It is important to also note that not all interaction decisions are the product of (or even align with)
220 a particular individual's risk tolerance, but rather are the combined product of individual decisions and
221 systemic social and workplace structures that constrain individual behaviour. This is a critical consideration
222 in the construction of policy, especially when such policies tend to be focused on individuals themselves
223 and (occasionally) those directly under their care, rather than a consideration of potential interactions with
224 (and consequent transmission risk to) other vulnerable individuals [44]. For instance, those with underlying
225 health conditions might be able to apply for remote work with a note from a medical provider, however,
226 they are less likely to be granted accommodation if their housemate is the vulnerable individual. Relatedly,
227 such policies have historically been applicable only after an individual is infected, rather than allow for the
228 reduction of transmission prophylactically. More effective protection of vulnerable individuals would require
229 facilitating household-wide action to reduce exposures [45, 46].

230 3.2 Quantifying the effect of population structure

231 Beyond individual risk-management, we found intrinsic differences in epidemic dynamics between populations
232 that differed in their age or household size distributions. Comparing a "Florida-like" population to a "Texas-
233 like" population (just "Florida" and "Texas", hereafter), we find consistent, slight differences in the maximum
234 proportion of the population concurrently infectious ("peak proportion infectious"; means of 16% *vs.* 17%,
235 respectively) and in the proportion of vulnerable individuals in the network that are infected over the course
236 of the epidemic (75% *vs.* 85%; fig. 2). Note that while vulnerable individuals make up a larger proportion
237 of the population, on average, in Florida (21% *vs.* 18% in Texas), we see a higher proportion of vulnerable
238 individuals getting infected in the Texas population. This is a result of the higher rate of spread (also
239 indicated by the higher peak proportion infectious) in the latter population, due in part to the larger average
240 household size (2.8 in Texas *vs.* 2.5 in Florida), and consequent higher number of strong within-household
241 interactions (table 1).

242 It is noteworthy that these small differences in peak proportion infectious and proportion of vulnerable
243 individuals infected were insufficient to fully counter the greater intrinsic mortality risk of the Florida pop-
244 ulation (6.2% of the population dying in the Florida population, 5.9% in Texas). This could be due, in part
245 to the counter-acting effects of age and household size distributions. In short, the household size distribution
246 of Texas tends to lead to larger outbreaks, but the larger proportion of vulnerable individuals in Florida
247 means that a similar number of individuals die despite fewer total people being infected.

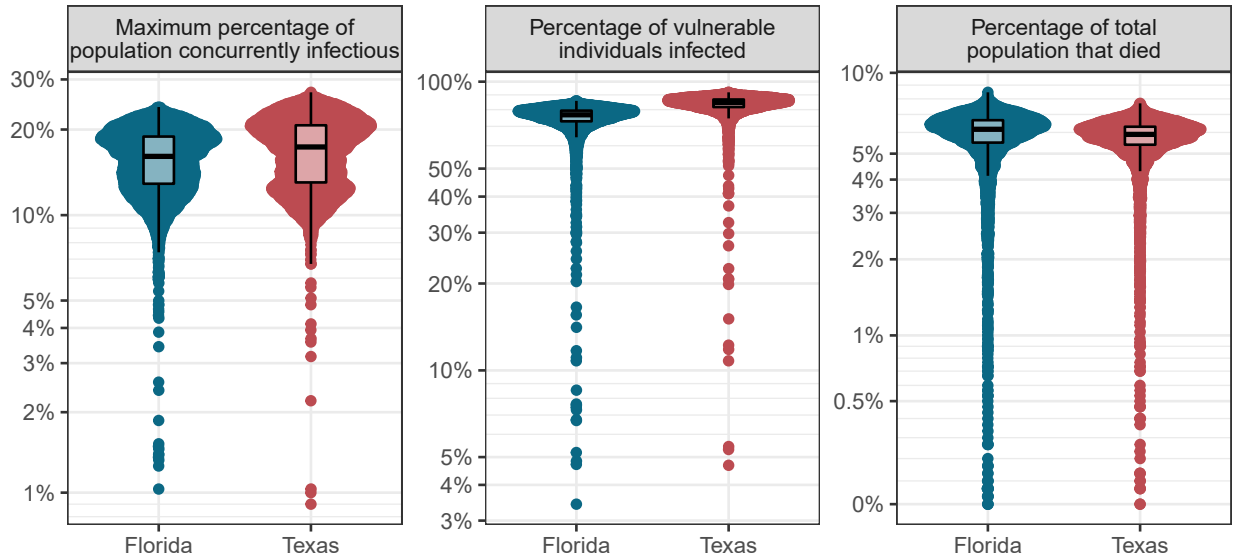


Figure 2: Comparing the difference in peak proportion infectious, overall prevalence among vulnerable individuals, and overall mortality between simulations of epidemics in two possible population structures, as characterized by age- and household-size distributions (see Electronic Supplementary Material and table 1). Florida has an (on average) older age distribution than Texas, while Texas has (on average) larger households. Each point represents a single simulated epidemic, conducted across a range of classmate- and co-worker transmission rates. Only simulations with no difference in behaviour based on vulnerability and only outcomes from epidemics resulting in greater than 5% of the total population being infected are shown (5 778 simulations for Florida, 6 297 for Texas). *N.b.* each panel has independent vertical axes limits. See Electronic Supplementary Material section S3 and figs. S3 and S7 for analogous figures under different background transmission rates and fig. S12 for alternative epidemiological outcome measures.

248 These results point to the importance of understanding trade-offs and nuances in population structure
249 when implementing public health interventions. For instance, when distributing effort to minimize lives-lost,
250 one must consider both properties of individuals in the population (*e.g.* what proportion of the population
251 is at increased vulnerability to adverse outcomes?) and properties of the social contact network that in-
252 terconnects those individuals (*e.g.* what are the most likely infection pathways by which those vulnerable
253 people can become infected?). The efficacy and cost efficiency of any public health efforts will depend on
254 understanding these nuances and their interaction. For instance, it may be more effective to isolate young
255 family members of vulnerable individuals than vulnerable individuals themselves, since the latter tend to be
256 older and have fewer social interactions to begin with [27].

257 Of course, the social and economic consequences of any intervention (which may be related to the total
258 number of interactions removed under intervention) must likewise be taken into consideration [47]. Criti-
259 cally, the effects of public policies have unequal effects across a population: school closure most negatively
260 affects less-educated families [48], wealthier individuals are more able to tolerate (and comply with) travel
261 restrictions [49, 47], and already marginalized communities often bear the brunt of adverse medical out-
262 comes [50]. Likewise, the distribution of underlying medical conditions is not distributed uniformly across
263 the population, often correlating with race and socio-economic status [51, 52]. Thus, an intervention focused
264 on (families of) vulnerable individuals, will necessarily also have disparate social and financial impact on
265 these already marginalized individuals. In short, while this study focuses on generic effects of contact net-
266 work structure on disease spread, real-world applications must additionally consider the specifics of which
267 individuals are affected by a policy decision.

268 3.3 Quantifying effects of interaction types

269 While it is difficult to disentangle the web of interactions that make up modern societies, we used linear
270 models to investigate the effects of a given change in interaction strength in one layer on the rate or extent
271 of disease spread in the population.

272 We found that a change in the co-worker transmission rate consistently resulted in a larger change in
273 epidemic outcome than a similarly sized change in the classmate transmission rate (fig. 3). For example, an
274 increase in co-worker transmission rate will have approximately twice the effect on peak proportion infectious,
275 total death burden, and time to that peak than will a similar increase in classmate transmission. When
276 considering the scenario of no change in behaviour based on vulnerability, this ratio climbs to approximately
277 3. Consistent with results in fig. 1, we saw smaller slopes (and reduced differences between the effects of

278 different network layers) for total number of deaths when households containing vulnerable individuals limited
279 exposure. Consistent with fig. 2, we saw that changes in transmission rates tended to have a larger effect
280 (*i.e.* model coefficient magnitude) on epidemic size in Texas, and on mortality in Florida (driven mostly by
281 workplace interactions).

282 This is driven in part by the difference in the number of interactions in the network associated with each
283 layer of the network. Because there are more individuals of working age than of school age, and because
284 workplaces can potentially be much larger than classrooms, there tends to be more co-worker interactions
285 in a given network than classmate interactions. While this is dependent upon the assumptions underlying
286 construction of these simulated contact networks, it is also generically true of the real human contact net-
287 works that inspired our approach. In most real-world societies, there are more working-age individuals than
288 children, and workplaces can potentially be orders of magnitude larger than school classrooms. The fact
289 that these results seem to be robust to imbalance in interaction strength suggests that network structure
290 (broadly construed) may have a larger role to play than pairwise interaction strength, at least for a highly
291 transmissible disease like COVID-19.

292 While the surface-level implication of these results is that efforts should be focused on workplaces, rather
293 than classrooms (and this is reinforced by evidence that, at least for early strains of SARS-CoV-2, trans-
294 mission to, from, and among children may be less than that among adults; [36, 53, 54, 55]), schools still
295 contribute meaningfully to disease spread, especially when considering some of the more recent (and more
296 transmissible) strains of SARS-CoV-2 [56]. Critically, alternative assumptions of mixing patterns could lead
297 to a different distribution of interactions between network layers. For instance, modelling schools as single
298 units and using age-structure to inform transmission rates between students (rather than clustering students
299 into discrete classroom units) produces networks with more classmate interactions than co-worker interac-
300 tions (Electronic Supplementary Material section S7, table S1). In these networks, classmate interactions
301 are therefore seen to be more consequential for some epidemiological outcomes, such as peak proportion
302 infectious, while for others co-worker interactions still have a greater effect, such as total number of individ-
303 uals infected (Electronic Supplementary Material fig. S15). It is also important to note that, in both cases,
304 the internal structure of workplace interaction networks are likewise highly connected. Compartmentalizing
305 workers, improving personal hygiene, ensuring adequate ventilation and air filtration, and supporting per-
306 sonal protective equipment usage can all alter the number and strength of interactions within the network.
307 Such interventions would reduce the overall impact of workplace interactions on disease spread.

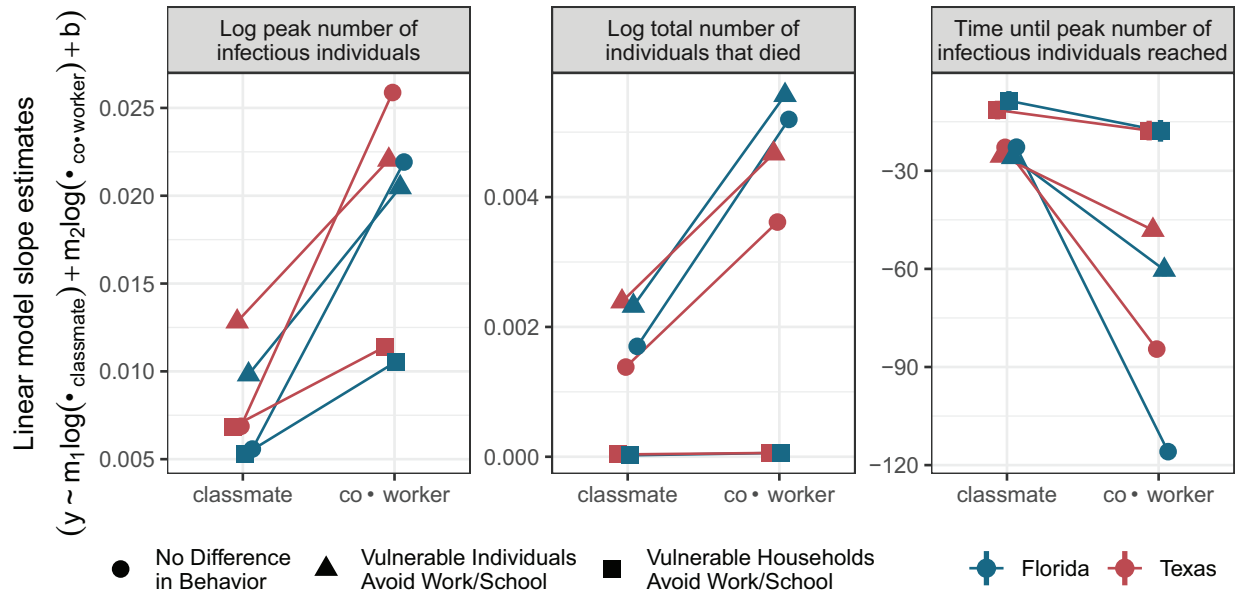


Figure 3: Quantifying the effect of changes in transmission rates on epidemic outcomes. The vertical axis indicates the value of the best-fitting coefficient for each transmission rate in a linear model of the form $y \sim m_1 \log(\beta_{\text{classmate}}) + m_2 \log(\beta_{\text{co-worker}}) + b$, where y indicates an epidemic outcome measure, m_n is a fitted slope coefficient, β_x represents a transmission rate for interaction type x , and b is a fitted intercept coefficient. The horizontal axis distinguishes between the two coefficients (m_1 : “classmate”, or m_2 : “co-worker”). Facets distinguish between epidemic outcome measures, point shapes distinguish risk-tolerance regimes (*i.e.* rows in fig. 1), and point colours distinguish age and household size distribution locales (as in fig. 2). Vertical lines extending beyond the point extents indicate 95% confidence intervals for the slope estimates (most confidence intervals are obscured by the points). To ease interpretation, lines connect coefficient values across interaction types for results from models of the same risk-tolerance regime and locale. Points are slightly offset horizontally to reduce overlap. Note that a more positive slope in the left and center facets indicates a greater number of individuals infectious or died, respectively, while a more negative slope in the right facet indicates a faster rate of infection (less time to reach peak infectiousness). Only outcomes from epidemics resulting in greater than 5% of the total population being infected were included in the linear models (13 182 simulations for Florida, 14 844 for Texas). *N.b.* each panel has independent vertical axes limits. See Electronic Supplementary Material section S3 and figs. S4 and S8 for analogous figures under different background transmission rates and fig. S13 for alternative epidemiological outcome measures.

308 4 Limitations & future directions

309 While the networks used in this study are inspired by empirical human contact networks, there were nonethe-
310 less many assumptions built into their construction that are necessarily unrealistic. Future studies could,
311 for example, consider differences in fine-scale network structure between interaction types, add additional
312 explicit interaction layers, and increase network size to better reflect a whole urban area. In particular,
313 one might nest individual classrooms within a less-strongly connected collection to represent a school, where
314 interactions can likewise occur in public spaces such as the cafeteria or library [26, 57]. Such interactions
315 are increasingly likely as schools relax their physical distancing requirements. Similarly, there might be
316 differences in between- and within-classroom structure for differently aged students. Within workplaces,
317 there might be a hierarchical network structure, where some peoples (*e.g.* managers) might interact with a
318 collection of individuals that otherwise have little interaction with one another. Finally, we focused on only
319 two types of interactions: those between classmates and those between co-workers. Clearly, there are myriad
320 other ways in which individuals interact with one another, each of which might be structured in unique ways.

321 Simulating disease upon interaction networks is, in general, computationally limited by the number of
322 edges in the network. To reduce simulation complexity and maximize modelled population sizes, we modelled
323 the fully-connected background transmission layer (in which every individual is connected to all others
324 in the population) implicitly as a prevalence-mediated risk of spontaneous infection at each timestep.
325 That is, the higher the community prevalence, the more likely an individual is to be infected by some
326 pathway other than the explicit connections in classrooms, workplaces, and households. In the Electronic
327 Supplementary Material (section S7), we consider an alternative construction, where background edges are
328 explicitly described by age-structured interactions [58]. In these simulations, we favoured age-structure over
329 compartmentalization as a guiding assumption for network construction, leading to more connected networks,
330 albeit with greater variation in interaction strength. Yet, this added realism (in some respects) comes with
331 a cost of a reduction in the maximally computationally-feasible population size. The ability to simulate
332 upon larger populations would moreover allow for additional levels of organization in our communities, for
333 instance considering the inherent compartmentalization of small towns distributed on a landscape.

334 This study was in part limited by available data sources. While national-level data is readily available
335 for most elements of our network generation, the same data for localities (even at the level of US states) is
336 less accessible. An additional consideration is covariance between different aspects of population structure,
337 where most data sources are segmented. For instance, one might assume that larger households have a lower
338 average age (*i.e.* more children), yet age and household-size distributions are only available independently

339 through the US Census American Community Survey.

340 In our disease model, we utilized disease parameters corresponding to the initial wave of COVID-19,
341 despite substantial strain evolution since that time. Because our focus in this work is not on any one disease
342 in particular, we opted to use an older strain for the increased availability and reliability of parameter
343 estimates. These literature-based parameters additionally result in mortality being almost exclusively among
344 vulnerable individuals—a trait we treated as binary and assigned based on post hoc empirical hospitalization
345 rates. A more robust approach would be to consider the distribution of specific underlying health conditions
346 within the population and their relative contribution to adverse outcomes. Critically, this approach also
347 assumes constant mortality rates, disregarding a known relationship in which increased hospital occupancy
348 results in worse disease outcomes [59].

349 **5 A note on generality**

350 In the midst of an ongoing pandemic of COVID-19, much of the inspiration for this work, and literature
351 referenced herein has considered this one disease in particular. Nevertheless, the results presented here stem
352 from a disease model that could be applied to many transmissible diseases with minimal modification. Even in
353 the consideration of SARS-CoV-2, as new strains arise, resulting in altered rates of transmission, progression,
354 recovery, and/or mortality, we expect the fundamental effects of network structure on disease spread to
355 persist. For instance, as COVID-19 mortality rates have sequentially declined over the past two years,
356 focus has shifted from mortality to hospitalization. As the drivers behind hospitalization and mortality are
357 largely equivalent [60, 61], one could apply this same framework in the context of hospitalization. Likewise,
358 vaccination (depending on efficacy) can be thought of as equivalent to either removing interactions (as in
359 isolation) or reducing interaction strength (as in increased mask usage). Thus, omitting consideration of the
360 additional benefits of reduced disease severity on the vaccinated individual, vaccination strategy could mirror
361 consideration of physical distancing recommendations in this work. Importantly, when reduction of disease
362 severity is additionally considered, previous work has suggested that prioritizing vulnerable individuals is
363 most efficacious [62].

364 **6 Conclusion**

365 Our simulations reinforce the consequences of our highly connected, modern society on disease spread. In
366 short, we find that decisions are rarely “personal” when it comes to public health, and the policies and health

367 decisions of a population can have dramatic effects of the spread of disease. Action by vulnerable individuals
368 in isolation does little to reduce their disease burden, suggesting that policies should additionally consider
369 the potential for next-order transmission to vulnerable individuals from the less-vulnerable individuals that
370 interact with them. Additionally, a population's composition and social contact network structure can
371 have marked effects on disease prevalence and mortality, though in our analysis these relationships were
372 slight and sometimes resulted in counter-intuitive results whereby rapid disease spread can counteract the
373 benefit of an otherwise less-vulnerable population. Finally, the structure of workplaces potentially provides
374 greater avenues for disease spread than do schools, but these effects are highly dependent on both how
375 workplaces/schools are structured, as well as the utilization and efficacy of non-pharmaceutical interventions
376 in each of these contexts.

377 While over-interpretation of specific values should be avoided in purely simulation-based studies such as
378 these, comparisons between different simulations can nevertheless provide insight into the relative importance
379 of different components of a contact network on the rate and extent of disease spread. By comparing
380 simulations across constrained axes of variation, such as types of interactions, differences in personal risk
381 tolerance (or systemic structures and policies), and different population structures, we glean insights into
382 how the different layers of social contact networks can have different levels of importance when it comes
383 to containing epidemic spread. We can use this nuanced understanding to better inform and differentiate
384 between public health strategies.

385 **7 Acknowledgements**

386 We thank Janine Mistrick, Chris Wojan, Emily Schafsteck, Desiree Walton, and Lisa Meyer for feedback on
387 early drafts of this work.

388 **8 Funding**

389 This work was supported by the National Science Foundation [DEB 1654609 and 2030509], a University of
390 Minnesota Office of Academic Clinical Affairs COVID-19 Rapid Response Grant, the Office of the Director,
391 National Institutes of Health [NIH T32OD010993], the University of Minnesota Informatics Institute Mn-
392 DRIVE program, the Van Sloun Foundation, and by the National Socio-Environmental Synthesis Center
393 (SESYNC) under funding received from the National Science Foundation [DBI 1639145]. The content is
394 solely the responsibility of the authors and does not necessarily represent the official views of the National

395 Institutes of Health.

396 References

- 397 1. Leung NH. Transmissibility and transmission of respiratory viruses. *Nat. Rev. Microbiol.* 2021; 19 (8)
398 :528–45. DOI: 10.1038/s41579-021-00535-6
- 399 2. Danon L, House TA, Read JM, and Keeling MJ. Social encounter networks: collective properties and
400 disease transmission. *J. Royal Soc. Interface* 2012; 9 (76) :2826–33. DOI: 10.1098/rsif.2012.0357
- 401 3. Harrison M. *Contagion: How Commerce Has Spread Disease*. Yale University Press, 2012
- 402 4. Huerta R and Tsimring LS. Contact tracing and epidemics control in social networks. *Phys. Rev. E*
403 2002; 66 (5) :056115. DOI: 10.1103/PhysRevE.66.056115
- 404 5. Morris M. Epidemiology and social networks: Modeling structured diffusion. *Sociol. Methods & Res.*
405 1993; 22 (1) :99–126. DOI: 10.1177/0049124193022001005
- 406 6. Danon L, Ford AP, House T, Jewell CP, Keeling MJ, Roberts GO, Ross JV, and Vernon MC. Networks
407 and the epidemiology of infectious disease. *Interdiscip. Perspect. on Infect. Dis.* 2011. DOI: 10.1155/
408 2011/284909
- 409 7. Nande A, Adlam B, Sheen J, Levy MZ, and Hill AL. Dynamics of COVID-19 under social distancing
410 measures are driven by transmission network structure. *PLOS Comput. Biol.* 2021; 17 (2) :e1008684.
411 DOI: 10.1371/journal.pcbi.1008684
- 412 8. Read JM and Keeling MJ. Disease evolution on networks: the role of contact structure. *Proc. Royal
413 Soc. B: Biol. Sci.* 2003; 270 (1516) :699–708. DOI: 10.1098/rspb.2002.2305
- 414 9. Ames GM, George DB, Hampson CP, Kanarek AR, McBee CD, Lockwood DR, Achter JD, and Webb
415 CT. Using network properties to predict disease dynamics on human contact networks. *Proc. Royal
416 Soc. B: Biol. Sci.* 2011; 278 (1724) :3544–50. DOI: 10.1098/rspb.2011.0290
- 417 10. Kamp C. Untangling the interplay between epidemic spread and transmission network dynamics. *PLOS
418 Comput. Biol.* 2010; 6 (11). DOI: 10.1371/journal.pcbi.1000984
- 419 11. Espinoza B, Castillo-Chavez C, and Perrings C. Mobility restrictions for the control of epidemics: When
420 do they work? *PLOS ONE* 2020; 15 (7) :e0235731. DOI: 10.1371/journal.pone.0235731
- 421 12. Camitz M and Liljeros F. The effect of travel restrictions on the spread of a moderately contagious
422 disease. *BMC Med.* 2006; 4 (1) :1–10. DOI: 10.1186/1741-7015-4-32

423 13. Aleta A, Martin-Corral D, Pastore y Piontti A, Ajelli M, Litvinova M, Chinazzi M, Dean NE, Halloran
424 ME, Longini Jr IM, Merler S, et al. Modelling the impact of testing, contact tracing and household
425 quarantine on second waves of COVID-19. *Nat. Hum. Behav.* 2020; 4 (9) :964–71. DOI: 10.1038/
426 s41562-020-0931-9

427 14. D’angelo D, Sinopoli A, Napoletano A, Gianola S, Castellini G, Del Monaco A, Fauci AJ, Latina R,
428 Iacobossi L, Salomone K, et al. Strategies to exiting the COVID-19 lockdown for workplace and school:
429 A scoping review. *Saf. Sci.* 2021; 134 :105067. DOI: 10.1016/j.ssci.2020.105067

430 15. Anderson RM, Heesterbeek H, Klinkenberg D, and Hollingsworth TD. How will country-based mitigation
431 measures influence the course of the COVID-19 epidemic? *The Lancet* 2020; 395 (10228) :931–4.
432 DOI: 10.1016/S0140-6736(20)30567-5

433 16. Glass RJ, Glass LM, Beyeler WE, and Min HJ. Targeted social distancing designs for pandemic in-
434 fluenza. *Emerg. Infect. Dis.* 2006; 12 (11) :1671. DOI: 10.3201/eid1211.060255

435 17. Koh WC, Naing L, and Wong J. Estimating the impact of physical distancing measures in containing
436 COVID-19: an empirical analysis. *Int. J. Infect. Dis.* 2020; 100 :42–9. DOI: 10.1016/j.ijid.2020.
437 08.026

438 18. Prakash N, Srivastava B, Singh S, Sharma S, and Jain S. Effectiveness of social distancing interventions
439 in containing COVID-19 incidence: International evidence using Kalman filter. *Econ. & Hum. Biol.*
440 2022; 44 :101091. DOI: 10.1016/j.ehb.2021.101091

441 19. Gardner BJ and Kilpatrick AM. Contact tracing efficiency, transmission heterogeneity, and accelerating
442 COVID-19 epidemics. *PLOS Comput. Biol.* 2021; 17 (6) :e1009122. DOI: 10.1371/journal.pcbi.
443 1009122

444 20. Kerr CC, Mistry D, Stuart RM, Rosenfeld K, Hart GR, Núñez RC, Cohen JA, Selvaraj P, Abeyseuriya
445 RG, Jastrzębski M, et al. Controlling COVID-19 via test-trace-quarantine. *Nat. Commun.* 2021; 12
446 (1) :1–12. DOI: 10.1038/s41467-021-23276-9

447 21. Chu DK, Akl EA, Duda S, Solo K, Yaacoub S, Schünemann HJ, El-harakeh A, Bognanni A, Lotfi
448 T, Loeb M, et al. Physical distancing, face masks, and eye protection to prevent person-to-person
449 transmission of SARS-CoV-2 and COVID-19: a systematic review and meta-analysis. *The Lancet* 2020;
450 395 (10242) :1973–87. DOI: 10.1016/j.jvs.2020.07.040

451 22. Howard J, Huang A, Li Z, Tufekci Z, Zdimal V, Westhuizen HM van der, Delft A von, Price A, Fridman
452 L, Tang LH, et al. An evidence review of face masks against COVID-19. *Proc. National Acad. Sci.* 2021;
453 118 (4). DOI: 10.1073/pnas.2014564118

454 23. Nofal AM, Cacciotti G, and Lee N. Who complies with COVID-19 transmission mitigation behavioral
455 guidelines? *PLOS ONE* 2020; 15 (10) :e0240396. DOI: 10.1371/journal.pone.0240396

456 24. Bavel JJV, Baicker K, Boggio PS, Capraro V, Cichocka A, Cikara M, Crockett MJ, Crum AJ, Dou-
457 glas KM, Druckman JN, et al. Using social and behavioural science to support COVID-19 pandemic
458 response. *Nat. Hum. Behav.* 2020; 4 (5) :460–71. DOI: 10.1038/s41562-020-0884-z

459 25. Singh AK, Gillies CL, Singh R, Singh A, Chudasama Y, Coles B, Seidu S, Zaccardi F, Davies MJ, and
460 Khunti K. Prevalence of co-morbidities and their association with mortality in patients with COVID-19:
461 a systematic review and meta-analysis. *Diabetes, Obes. Metab.* 2020; 22 (10) :1915–24. DOI: 10.1111/
462 dom.14124

463 26. Meyers LA, Pourbohloul B, Newman ME, Skowronski DM, and Brunham RC. Network theory and
464 SARS: predicting outbreak diversity. *J. Theor. Biol.* 2005; 232 (1) :71–81. DOI: 10.1016/j.jtbi.
465 2004.07.026

466 27. Prem K, Cook AR, and Jit M. Projecting social contact matrices in 152 countries using contact surveys
467 and demographic data. *PLOS Comput. Biol.* 2017; 13 (9) :e1005697. DOI: 10.1371/journal.pcbi.
468 1005697

469 28. Manout O and Ciari F. Assessing the role of daily activities and mobility in the spread of COVID-19 in
470 Montreal with an agent-based approach. *Front. Built Environ.* 2021 :101. DOI: 10.3389/fbuil.2021.
471 654279

472 29. Halloran ME, Ferguson NM, Eubank S, Longini Jr IM, Cummings DA, Lewis B, Xu S, Fraser C,
473 Vullikanti A, Germann TC, et al. Modeling targeted layered containment of an influenza pandemic in
474 the United States. *Proc. National Acad. Sci.* 2008; 105 (12) :4639–44. DOI: 10.1073/pnas.0706849105

475 30. U.S. Census Bureau. S2501: Occupancy Characteristics. American Community Survey 1-Year Es-
476 timates. 2019. Available from: https://data.census.gov/cedsci/table?q=texas%20household%20size%20distribution&g=0100000US_0400000US12&tid=ACSST1Y2019.S2501

477 31. U.S. Census Bureau. DP05: ACS Demographic and Housing Estimates. American Community Sur-
478 vey 1-Year Estimates. 2019. Available from: <https://data.census.gov/cedsci/table?q=age%20distribution&g=0100000US%240400000&tid=ACSDP1Y2019.DP05>

481 32. CDC COVID-19 Response Team, Bialek S, Boundy E, Bowen V, Chow N, Cohn A, Dowling N, Ellington
482 S, Gierke R, Hall A, et al. Severe outcomes among patients with coronavirus disease 2019 (COVID-
483 19)—United States, February 12–March 16, 2020. *Morb. Mortal. Wkly. Rep.* 2020; 69 (12) :343. DOI:
484 10.15585/mmwr.mm6912e2

485 33. Bailey NTJ. The mathematical theory of epidemics. eng. New York: Hafner Publishing Company, 1957

486 34. Bar-On YM, Flamholz A, Phillips R, and Milo R. Science Forum: SARS-CoV-2 (COVID-19) by the
487 numbers. *eLife* 2020; 9 :e57309

488 35. Linton NM, Kobayashi T, Yang Y, Hayashi K, Akhmetzhanov AR, Jung Sm, Yuan B, Kinoshita R,
489 and Nishiura H. Incubation period and other epidemiological characteristics of 2019 novel coronavirus
490 infections with right truncation: a statistical analysis of publicly available case data. *J. Clin. Med.*
491 2020; 9 (2) :538. DOI: 10.3390/jcm9020538

492 36. Rosenberg ES, Dufort EM, Blog DS, Hall EW, Hoefer D, Backenson BP, Muse AT, Kirkwood JN,
493 St. George K, Holtgrave DR, et al. COVID-19 testing, epidemic features, hospital outcomes, and
494 household prevalence, New York State—March 2020. *Clin. Infect. Dis.* 2020; 71 (8) :1953–9. DOI:
495 10.1093/cid/ciaa549

496 37. Bar-On YM, Sender R, Flamholz AI, Phillips R, and Milo R. A quantitative compendium of COVID-19
497 epidemiology. *arXiv preprint arXiv:2006.01283* 2020. DOI: 10.48550/arXiv.2006.01283

498 38. Wang Y, Kang H, Liu X, and Tong Z. Asymptomatic cases with SARS-CoV-2 infection. *J. Med. Virol.*
499 2020; 92 (9) :1401–3. DOI: 10.1002/jmv.25990

500 39. The World Bank. Life expectancy. 2022. Available from: <https://data.worldbank.org/indicator/SP.DYN.LE00.IN?locations=XD>

501 40. Ugarte MP, Achilleos S, Quattrocchi A, Gabel J, Kolokotroni O, Constantinou C, Nicolaou N, Rodriguez-
502 Llanes JM, Huang Q, Verstiuk O, et al. Premature mortality attributable to COVID-19: potential years
503 of life lost in 17 countries around the world, January–August 2020. *BMC Public Health* 2022; 22 (1)
504 :1–13. DOI: 10.1186/s12889-021-12377-1

505 41. Wu J, Dhingra R, Gambhir M, and Remais JV. Sensitivity analysis of infectious disease models:
506 methods, advances and their application. *J. The Royal Soc. Interface* 2013; 10 (86) :20121018. DOI:
507 10.1098/rsif.2012.1018

508 42. R Core Team. R: A Language and Environment for Statistical Computing. R Foundation for Statistical
509 Computing. Vienna, Austria, 2022. Available from: <https://www.R-project.org/>

511 43. National Center for Health Statistics. Conditions Contributing to COVID-19 Deaths, by State and
512 Age, Provisional 2020–2022. 2022. Available from: <https://data.cdc.gov/NCHS/Conditions-Contributing-to-COVID-19-Deaths-by-Stat/hk9y-quqm>

514 44. Mayer G. The family and medical leave act (FMLA): Policy issues. Library of Congress Washington
515 DC Congressional Research Service. 2013

516 45. Wu JT, Riley S, Fraser C, and Leung GM. Reducing the impact of the next influenza pandemic using
517 household-based public health interventions. *PLOS Med.* 2006; 3 (9) :e361. DOI: 10.1371/journal.
518 pmed.0030361

519 46. House T and Keeling M. Household structure and infectious disease transmission. *Epidemiol. & Infect.*
520 2009; 137 (5) :654–61. DOI: 10.1017/S0950268808001416

521 47. Bonaccorsi G, Pierri F, Cinelli M, Flori A, Galeazzi A, Porcelli F, Schmidt AL, Valensise CM, Scala
522 A, Quattrociocchi W, et al. Economic and social consequences of human mobility restrictions under
523 COVID-19. *Proc. National Acad. Sci.* 2020; 117 (27) :15530–5. DOI: 10.1073/pnas.2007658117

524 48. Engzell P, Frey A, and Verhagen MD. Learning loss due to school closures during the COVID-19
525 pandemic. *Proc. National Acad. Sci.* 2021; 118 (17) :e2022376118. DOI: 10.1073/pnas.2022376118

526 49. Iio K, Guo X, Kong X, Rees K, and Wang XB. COVID-19 and social distancing: Disparities in mobility
527 adaptation between income groups. *Transp. Res. Interdiscip. Perspect.* 2021; 10 :100333. DOI: 10.
528 1016/j.trip.2021.100333

529 50. Tan SB, DeSouza P, and Raifman M. Structural racism and COVID-19 in the USA: a county-level
530 empirical analysis. *J. Racial Ethn. Health Disparities* 2022; 9 (1) :236–46. DOI: 10.1007/s40615-020-
531 00948-8

532 51. Kabarriti R, Brodin NP, Maron MI, Guha C, Kalnicki S, Garg MK, and Racine AD. Association
533 of race and ethnicity with comorbidities and survival among patients with COVID-19 at an urban
534 medical center in New York. *JAMA network open* 2020; 3 (9) :e2019795–e2019795. DOI: 10.1001/jamanetworkopen.2020.19795

536 52. Seligman B, Ferranna M, and Bloom DE. Social determinants of mortality from COVID-19: A simu-
537 lation study using NHANES. *PLoS medicine* 2021; 18 (1) :e1003490. DOI: 10.1371/journal.pmed.
538 1003490

539 53. Li W, Zhang B, Lu J, Liu S, Chang Z, Peng C, Liu X, Zhang P, Ling Y, Tao K, et al. Characteristics
540 of household transmission of COVID-19. *Clin. Infect. Dis.* 2020; 71 (8) :1943–6. DOI: 10.1093/cid/
541 ciaa450

542 54. Lei H, Xu X, Xiao S, Wu X, and Shu Y. Household transmission of COVID-19-a systematic review and
543 meta-analysis. *J. Infect.* 2020; 81 (6) :979–97. DOI: 10.1016/j.jinf.2020.08.033

544 55. Madewell ZJ, Yang Y, Longini IM, Halloran ME, and Dean NE. Factors associated with household
545 transmission of SARS-CoV-2: an updated systematic review and meta-analysis. *JAMA Netw. Open*
546 2021; 4 (8) :e2122240–e2122240. DOI: 10.1001/jamanetworkopen.2021.22240

547 56. Dawood FS, Porucznik CA, Veguilla V, Stanford JB, Duque J, Rolfs MA, Dixon A, Thind P, Hacker E,
548 Castro MJE, et al. Incidence rates, household infection risk, and clinical characteristics of SARS-CoV-2
549 infection among children and adults in Utah and New York City, New York. *JAMA Pediatr.* 2022; 176
550 (1) :59–67. DOI: 10.1001/jamapediatrics.2021.4217

551 57. Bilinski A, Salomon JA, Giardina J, Ciaranello A, and Fitzpatrick MC. Passing the test: a model-
552 based analysis of safe school-reopening strategies. *Ann. internal medicine* 2021; 174 (8) :1090–100.
553 DOI: 10.7326/M21-0600

554 58. Prem K, Zandvoort Kv, Klepac P, Eggo RM, Davies NG, Mathematical Modelling of Infectious Dis-
555 eases COVID-19 Working Group C for the, Cook AR, and Jit M. Projecting contact matrices in 177
556 geographical regions: an update and comparison with empirical data for the COVID-19 era. *PLoS*
557 *computational biology* 2021; 17 (7) :e1009098. DOI: 10.1371/journal.pcbi.1009098

558 59. Rossman H, Meir T, Somer J, Shilo S, Gutman R, Ben Arie A, Segal E, Shalit U, and Gorfine M.
559 Hospital load and increased COVID-19 related mortality in Israel. *Nat. Commun.* 2021; 12 (1) :1–7.
560 DOI: 10.1038/s41467-021-22214-z

561 60. Estiri H, Strasser ZH, and Murphy SN. Individualized prediction of COVID-19 adverse outcomes with
562 MLHO. *Sci. Reports* 2021; 11 (1) :1–9. DOI: 10.1038/s41598-021-84781-x

563 61. Moreira A, Chorath K, Rajasekaran K, Burmeister F, Ahmed M, and Moreira A. Demographic predic-
564 tors of hospitalization and mortality in US children with COVID-19. *Eur. J. Pediatr.* 2021; 180 (5)
565 :1659–63. DOI: 10.1007/s00431-021-03955-x

566 62. Bubar KM, Reinholt K, Kissler SM, Lipsitch M, Cobey S, Grad YH, and Larremore DB. Model-
567 informed COVID-19 vaccine prioritization strategies by age and serostatus. *Science* 2021; 371 (6532)
568 :916–21. DOI: 10.1126/science.abe6959